Application of deep learning algorithm for estimating stand volume in South Korea

Sungeun Cha [a,b], Hyun-Woo Jo [b], Moonil Kim [c], Cholho Song [d], Halim Lee [e], Eunbeen Park [b], Joongbin Lim [a], Dmitry Schepaschenko [f,g], Anatoly Shvidenko [f], Woo-Kyun Lee [b,d,*]

[a] National Institute of Forest Science, Forest ICT Center, Seoul, Republic of Korea
[b] Korea University, Department of Environmental Science and Ecological Engineering, Seoul, Republic of Korea
[c] Pyeongtaek University, Department of Integrated Environmental Systems, Pyeongtaek, Republic of Korea
[d] Korea University, OJEong Resilience Institute (OJERI), Seoul, Republic of Korea
[e] Institute for Integrated Management of Matter Fluxes and of Resource, United Nations University–UNU-FLORES, Dresden, Germany
[f] International Institute for Applied Systems Analysis (IIASA), Ecosystems Services and Management, Laxenburg, Austria
[g] Siberian Federal University, Krasnoyarsk, Russia

Abstract. Current estimates of stand volume for South Korean forests are mostly derived from expensive field data. Techniques that allow reducing the amount of ground data with reliable accuracy would decrease the cost and time. The fifth National Forest Inventory (NFI) has been conducted annually for all forest areas in South Korea from 2006 to 2010 and using these data we can make a model for estimating the stand volume of forests. The purpose of this study is to test deep learning whether it is available for measurement of stand volume with satellite imageries and geospatial information. The spatial distribution of the stand volume of South Korean forests was predicted with the convolutional neural networks (CNNs) algorithm. NFI data were randomly sampled for training from 90% to 10%, with 10% decrement, and the rest of the area was estimated using satellite imagery and geospatial information. Consequently, we found that the error rate of total stand volume was <5% when using over 17% of NFI data for training (R^2 ¼ 0.96). We identified that using CNNs model based on satellite imageries and geospatial information is considered to be suitable for estimating the national level of stand volume. This study is meaningful in that we (1) estimated the stand volume using a deep learning algorithm with high accuracy compare with previous studies, (2) identified the minimum training rate of the CNNs model to estimate the stand volume of South Korean forest, and (3) identified the effect of diameter class on error hotspots in stand volume estimates through clustering analysis.

Keywords: stand volume estimation; convolutional neural networks; national level of stand volume; satellite imageries; geospatial information.

1 Introduction

As an important part of terrestrial ecosystems, forest ecosystems are a huge global carbon pool and will likely play a long-term and sustained role in mitigating the impacts of global warming [1]. In South Korea, >63% of the country is covered by forest, which is twice the world average of 31%, and it has the fourth-largest forest area among Organization for Economic Co-operation and Development countries [2]; thus, an accurate estimation of stand volume is essential in understanding the carbon pool. The necessity for accurate estimates of forest stand volume is increasing nowadays due to the importance of sustainable forest management along with the assessment of forest structure, productivity, and carbon fluxes based on sequential changes in stand volume [3].

Estimating forest stand volume in South Korea is mostly conducted using both the Sampling method, which estimates the total population through a sampling survey and the Wall-to-Wall method, which can determine the land change of the total area in space units [4]. Korean National Forest Inventory (NFI) is mainly estimated using sampling techniques. The NFI, field surveyed data, includes various information such as tree species, tree height, diameter at breast height (DBH), stand volume, and the location of the surveyed area collected from entire forests in South Korea in the past for every 5 years [5]. Since the current stand volume estimation carried out by the Korean government costs >3 million dollars per year, there is a limitation in that it is difficult to conduct a survey on the entire forest nationwide annually considering the large budget required for a single survey [6]. To overcome these limitations, various methods have been developed to estimate stand volume [7]. Particularly, remote sensing technologies using satellite imagery such as KOMPSAT, LANDSAT, SENTINEL, and MODIS have become popular alternatives for estimating stand volume using various imaging methods [8–11]. In this regard, the satellite for forestry and agriculture (CAS500-4) scheduled to be launched in 2025 in Korea is expected to have great utility in estimating the national stand volume [12]. The aforementioned remote sensing imageries are convenient for obtaining the distribution of the forest stand. However, the actual problems related to the ground forest sample, such as estimation of the stand volume of accumulation in the sample, cannot be solved. To solve the problem, various data must be analyzed by complex expressions such as deep learning.

Deep learning is a technique of machine learning that refers primarily to artificial neural networks (ANNs) of sufficient complexity to interpret raw data without the need for human-derived explanatory variables [13]. Deep learning created major advances in solving problems that have resisted the best attempts of the artificial intelligence community for many years. It has turned out to show better performance in discovering intricate structures in high-dimensional data and is, therefore, applicable to many domains of environmental sectors [14].

Convolutional neural networks (CNNs) are greatly effective in large-scale image recognition, object detection, and semantic segmentation [15]. Some studies started using deep learning for measuring and analyzing forest attributes. For instance, Ref. 16 used a segmentation technique to isolate tree crowns, and a neural network (NN) to classify species based on point distribution. Reference 17 showed estimating improvements from 98.2% to 99.5% accuracy of three-dimensional (3D)-printed polymer using both support vector machine (SVM) and CNNs.

The purpose of this study is to test whether CNNs are available for measurement of stand volume under different environmental conditions such as variance in the wavelength of satellite imagery or geospatial information and to identify the minimum portion of the training data set for estimating the total amount of stand volume in South Korean forest.

2 Materials and Methods

2.1 *Study Area*

This study covered the whole of South Korea, which is in the midlatitude region (33°N to 38°N) in East Asia. The forest in South Korea is generally covered with a temperate forest; however, subtropical evergreen forests are found on the southern coast. Although the Korean peninsula has a very high rate of urbanization, forests still account for the highest land coverage (>60%) [18]. Figure 1 shows the study area and the distribution of forest cover in South Korea.

2.2 *Satellite Imageries and Geospatial Information for CNNs Model*

2.2.1 *National Forest Inventory data*

Estimation models using remote sensing must be accompanied by field data [19]. The IPCC Good Practice Guidance also suggests the need for accurate field survey data for estimating stand volume through remote sensing [20]. NFI data are field survey data from South Korea, which has been used for various studies to estimate stand volume [21]. The fifth NFI has been conducted annually for all forest areas in South Korea from 2006 to 2010. These data were collected by dividing the grid into 4 km units and placing systematic sampling points at the intersection points. Approximately 6200 plots were created for the entire South Korean terrestrial area, and ~4000 plots have been placed in the forest area since 1973. The NFI data provide a calculated stand volume from the measured data, such as tree height, DBH, and forest density (Nha). NFI data use the tree height curve and stand characteristics according to the stratified sample points based on the sample point research data to calculate the stand volume.

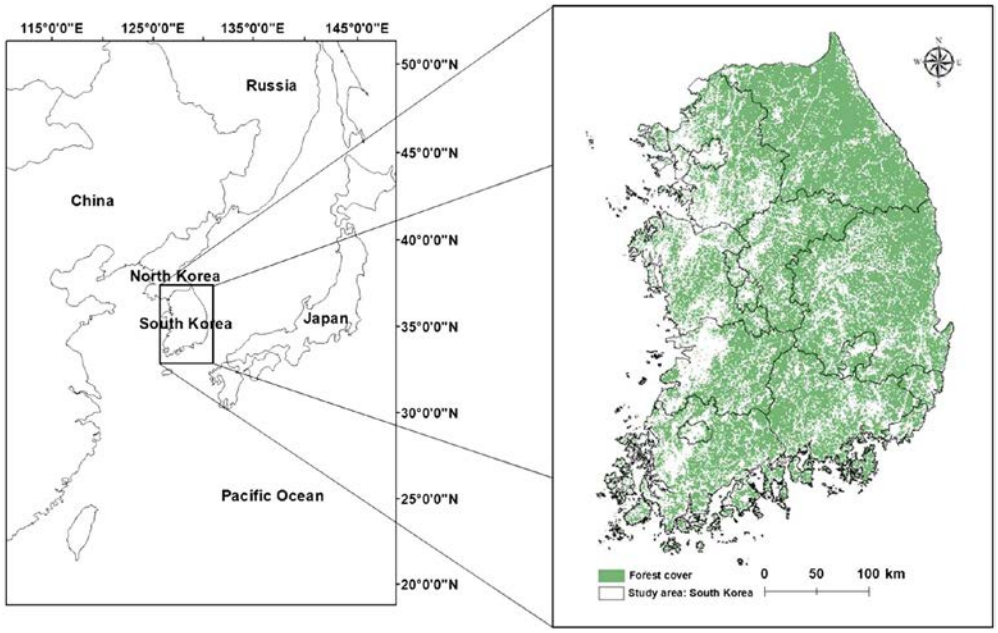

Fig. 1 The boundary of the study area including forest cover in South Korea.

The fixed sample point is composed of four subplots as a cluster plot. Additional sampling points are arranged in three directions: north (0 deg), 120 deg, and 240 deg, which are located 50-m away, centered on the origin of the sampling point (Fig. 2). The stand volume per unit area was calculated by classifying the basic research investigator (0.04 ha) by subplot and the large tree investigator (0.08 ha).

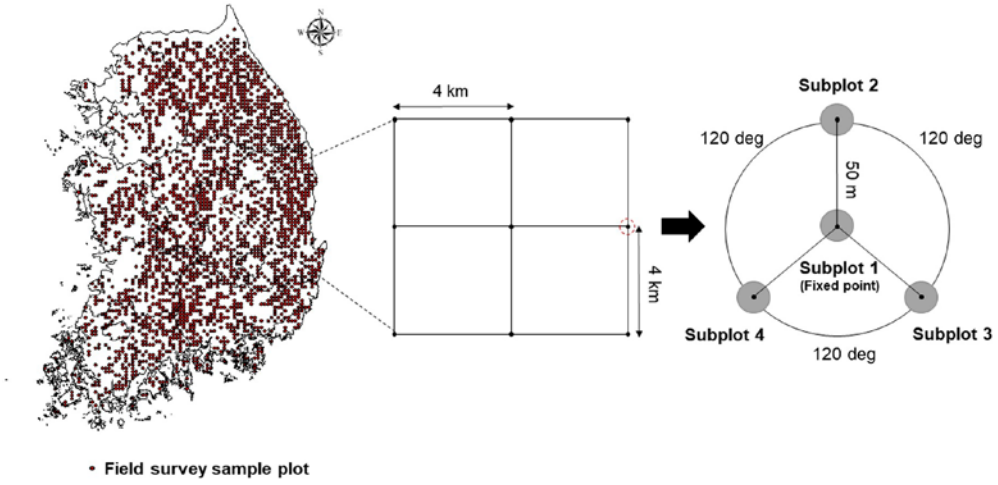

Fig. 2 Plot systems for the fifth NFI (modified from the original by Ref. 5).

The field surveyed data from neighboring subplots 2, 3, and 4 are stored in subplot 1 (fixed point) to represent the stand volume of the sample point. Within the sample point, DBH is measured only in timbers >6 cm. On the other hand, the height of the trees (h) is measured in the selected timber from the dominant tree species. The value of the stand volume was considered with the correlation between DBH and the tree height values.

2.2.2 *MODIS imageries*

We used MODIS version 6 products (MOD13A1: 16-day interval with the 250-m resolution, and MCD15A2H: 8-day interval with 500-m resolution), specifically the blue, red, NIR, and MIR reflectance, to reflect the effect of the wavelength on stand volume. Additionally, we used vegetation indices, which represent vegetation greenness, such as normalized difference vegetation index (NDVI) and enhanced vegetation index (EVI), the combined fraction of photosynthetically active radiation, and leaf area index (LAI) to increase the accuracy of stand volume estimation. Table 1 lists the MODIS data set used in this study. As NFI data were surveyed from 2006 to 2010, MODIS data were also collected from the same period. To reflect the effect of seasonal differences in stand volume estimation, we collected 720 imageries (eight layers × two times per month × 12 months × 5 years), which were averaged monthly.

2.2.3 *Geospatial information*

Topographic factors and forest types were used to reflect the effect of geospatial information on stand volume (Fig. 3). A digital map (1:5000) provided by the National Geographic Information Institute produced an elevation (digital terrain model) and slope map with 500-m spatial resolution. The area of broad-leaf, needle-leaf, and mixed forests was extracted using the land cover map provided by the Korean Ministry of Environment (ME). In the case of forest cover, the needle-leaf forest composition is dominated by *Pinus densiflor*, *Pinus koraiensis*, *Larix kaempferi (Lamb.) Carriere*, and *Pinus rigida*. On the other hand, the broad-leaf forest is mostly composed of *Quercus*, *Populus*, and *Castanea crenata*.

Table 1 Specification of MODIS data sets.

MODIS product	Layer name	Units	Spatial resolution	Data type
MOD13A1	NDVI	Dimensionless	250 m	16-bit signed integer
	EVI			
	Blue band	Reflectance		
	Red band			
	NIR band			
	MIR band			
MCD15A2H	LAI	Dimensionless	500 m	16-bit signed integer

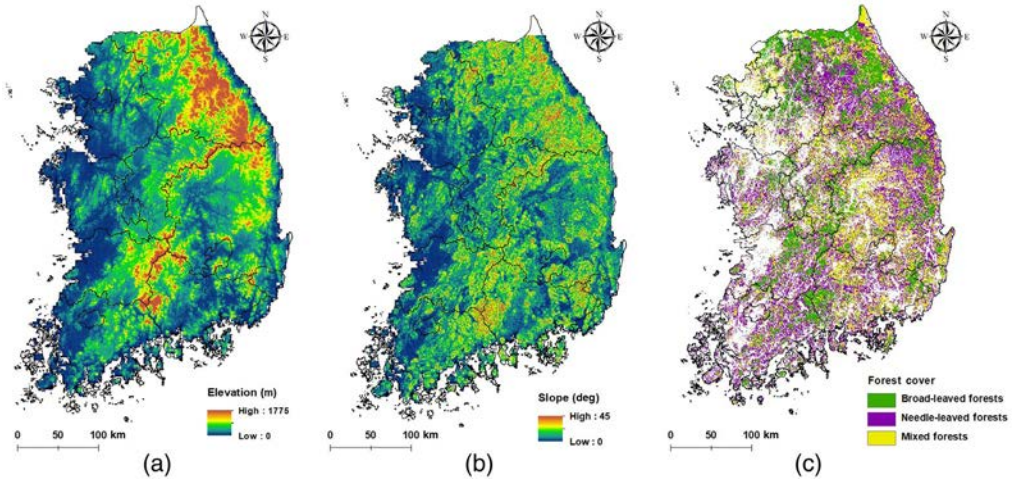

Fig. 3 Topographic factors and forest cover map: (a) elevation, (b) slope, and (c) forest cover.

2.3 *Data Processing*

2.3.1 *Algorithms of convolutional neural networks*

ANNs are biologically-inspired variants of multilayer-perceptron type NN s where the individual neurons respond to overlapping regions in the visible field [22]. This ANN is a model composed of multiple nested models using linear regression, such as SVM. NNs are typically composed of input layers, hidden layers, and output layers. CNNs, similarly layer-structured with typical NNs, are largely different in the way that the form of data used as input is specialized for the image.

The basic concept of CNNs is to allow each element of the filter, that is a matrix to be trained automatically for suitable data processing. CNNs receive data in the form of a matrix, so the form of the image is preserved [22]. Instead of creating all connections between layers, CNNs are only partially connected (sparse weight), and instead of updating the weight individually, certain weight groups share parameters so that the weight values within the group are always the same (parameter sharing). CNNs aim to enable automatically learning in selecting filters that maximize classification accuracy.

CNNs add a layer called a convolutional layer and a pooling layer in front of the fully connected layer. This is the way the model is trained to filter the original image using kernels before classification operation [23]. The convolutional layer

extracts the features of the input data by applying the kernel to the input image, and the pooling layer converts the calculated matrix values into one representative scalar value (the average of each element value of the matrix) to reduce the size of the image. Image data can be expressed as a 3D matrix (or "tensor") of height, width, and channels. In the data that have gone through padding, the parts including the certain features are shown in relatively large values, while the those without the features are shown as values close to 0. The activation function (rectified linear unit, ReLU) performs the task of changing the features, which turns out to be the output of the final convolution layer.

Figure 4 shows our CNNs configuration. we used four convolutional layers with the receptive field size of 3×3 and stride 1. The number of the channels was increased to 16, 32, 64, and 128 for the first to fourth channels, respectively. The batch normalization and max-pooling were performed between each step, and finally, the channel size was reduced to 64, 16, and 8 flattened to obtain the final output.

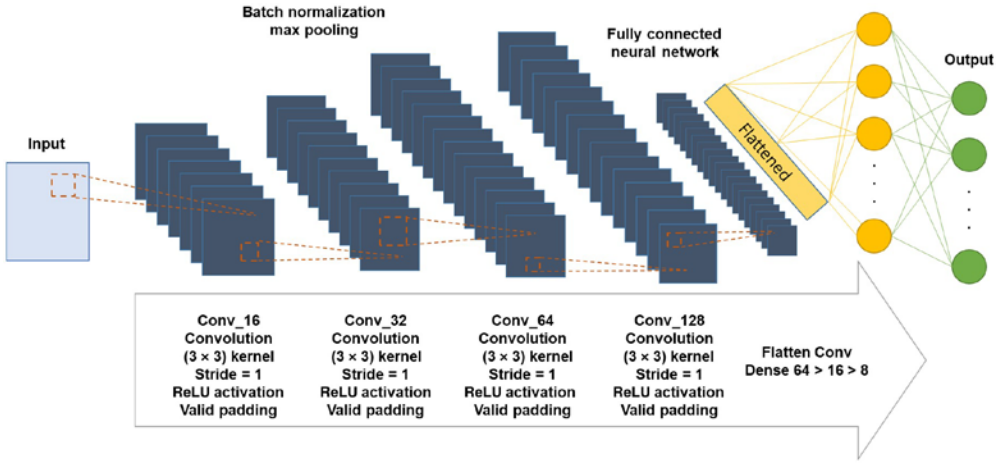

Fig. 4 Configuration of CNNs.

The CNNs algorithm was uniquely coded in python without any supplementary programming software. The main packages and versions used in python are Keras v.2.3.0 (Dense, Dropout, Activation, Flatten, Conv2D, MaxPooling2D, BatchNormalization, LSTM, and AveragePooling2D), TensorFlow v2.0, NumPy v.1.17.0.

2.3.2 *Identifying the characteristics by Moran's I statistical analysis and hotspot analysis*

Stand volume was estimated using various satellite imageries and geospatial information. Stand volume estimates using CNNs algorithm were calculated by reflecting the correlation of factors used; however, identifying the cluster of errors should be a priority to determine the reason for the errors. Thus, in this study, clusters of pixel-based errors were obtained through Moran's I statistical analysis. Moran's I is a quantitative index that compares the attributes of the target and neighboring objects to the mean of the overall data set as a statistic to measure the similarity of neighboring objects [24]. The range of the Moran's I value is from -1 to 1 [Eq. (1)]. A value >0 indicates that the spatial distribution of the analyzed target is a clustered pattern, <0 indicates a dispersed pattern, and closer to 0 indicates a random pattern. In this study, Moran's I value was calculated to identify the variance of the error in each pixel for the results of 17% training with 83% validation of the field survey data (NFI). In Eq. (1), $w_{i;j}$ represents the spatial weight between feature i and j, while n represents the total number of features

$$\text{Moran's I} = \frac{n \sum_i \sum_j w_{i,j}(x_i - \overline{x})(x_j - \overline{x})}{\sum_i \sum_j w_{i,j} \sum_i (x_i - \overline{x})^2}. \quad (1)$$

The causes of errors were analyzed according to the spatial distribution patterns of errors in stand volume estimates. Hotspot analysis reveals where the errors are clustered, and statistically compares the DBH at the location to determine why the error appears. Hotspot analysis is a statistical technique developed by Ref. 25 and is a method of expressing environmental variables spatially in clustered or dispersed regions [26,27]. G_i in Eq. (2) is the expression used to calculate the z-score for the error of stand volume estimation.

In Eq. (2), X represents the population mean of the error of stand volume estimation. S indicates the standard deviation for

the population mean, n represents the total number of errors, and x_j, j, $w_{i;j}$ represent the space weight between i and j. Besides, a value of Z-score >1.65 (p-value < 0.10) indicates a hotspot and a value of Z-score <−1.65 (p-value < 0.10) indicates a coldspot.

$$G_i = \frac{\sum_{j=1}^{n} w_{i,j} w_j - \overline{X} \sum_{j=1}^{n} w_{i,j}}{\sqrt{\frac{n \sum_{j=1}^{n} w_{i,j}^2 - \left(\sum_{j=1}^{n} w_{i,j}\right)^2}{n-1}}} \quad \overline{X} = \frac{\sum_{j=1}^{n} x_j}{n} \quad S = \sqrt{\frac{\sum_{j=1}^{n} x_j^2}{n} - (\overline{X})^2}. \tag{2}$$

The diameter class extracted from the NFI was used to analyze the spatial pattern of places where errors are concentrated for stand volume estimation. The diameter of stands was expressed as "diameter class" (small DBH: 0 to 16 cm, medium DBH: 16 to 30 cm, large DBH: over 30 cm).

3 Results and Discussion

3.1 *Stand Volume Estimation Using CNNs Model in South Korea*

We assigned an ID to each pixel to run the CNNs model. After that, the pixels were classified into a training data set for the learning, a validation data set for tuning hyperparameters and validating the model, and a test data set for testing the model after an initial inspection of the model with validation. In this study, data was split using "sklearn.neural_network" considering that all the data from a single plot should be part of a single data set (training, validation, or test data set) (Sec. 6.1).

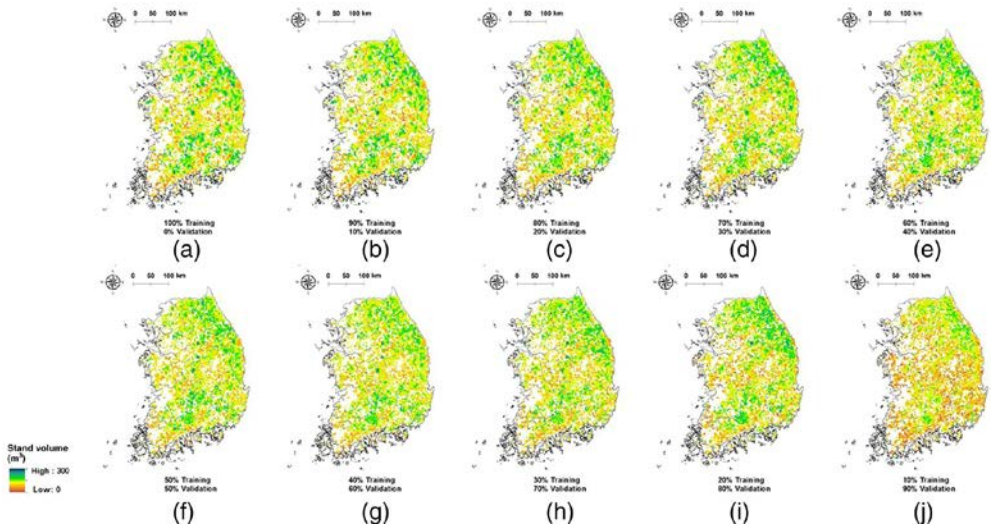

Fig. 5 The results of pixel-based stand volume map: (a) NFI data, (b) 90% training, 10% validation and test, (c) 80% training, 20% validation and test, (d) 70% training, 30% validation and test, (e) 60% training, 40% validation and test, (f) 50% training, 50% validation and test, (g) 40% training, 60% validation and test, (h) 30% training, 70% validation and test, (i) 20% training, 80% validation and test, and (j) 10% training, 90% validation and test.

In the field surveyed data (the NFI data), the stand volume distribution of all forests in Korea was on average 127.85 m^3 ha^{-1}, with a maximum of 275.71 m^3 ha^{-1}, a minimum of 21.47 m^3 ha^{-1}, and a total stand volume of 727.42 Mm^3. In this study, we assumed that the NFI data based on the field survey is the true value of the stand volume. The results of the analysis revealed that validation accuracy exceeded 92% when trained over 20% as shown in Figs. 5(a)–5(i) and all the test accuracy was >95%. However, when 10% was used for training and 90% was used for validation as shown in the red box in Fig. 5(j), the estimated total stand volume was 563.44 Mm^3 and the validation accuracy dramatically decreased to 57% (Fig. 6, Sec. 6.2). In this study, as we tried to determine the minimum percentage of training data required to estimate the forest stand volume of South Korea, the CNNs model was run at 10% to 20% training at 1% increment. When using 17% NFI data for training, the stand volume distribution was calculated to be 124.62 m^3 ha^{-1} with a total stand volume of 709.04 Mm^3 at 96% of validation accuracy, while using 16% NFI data for training showed 61% of validation accuracy (Fig. 7). Thus, stand volume

estimates for the entire forest is found assessable if a field survey including 1.1 million ha of the forest is conducted, considering that the forest area of South Korea is about 6.4 Mha [28].

3.2 *Forest Statistics Trends through Clustering Analysis*

We performed cluster analysis on the results of 17% training to estimate which part of growth characteristics could affect the stand volume. Moran's I value for the entire forest in South Korea was 0.16, which indicates that errors for stand volume estimates are clustered. Given the *z*-score of 33.14, there is a <1% likelihood that this clustered pattern could be the result of a random chance [29]. The distance threshold of spatial autocorrelation analyzed through Moran's I statistical analysis was applied at 14,423.65 m. Figure 8 shows the results of a hotspot analysis that indicates where the distributed errors are concentrated considering spatial autocorrelation. The meaning of a hotspot in this study is that the error is underestimated, and a coldspot indicates that the error is overestimated. In the forests of South Korea, while hotspots are distributed in a relatively sparse forest, coldspots are highly distributed in the northeastern Taebaek Mountains, where forests are concentrated.

The effects of diameter class on hotspot-concentrated areas are presented in Table 2. In the small class (0 to 16 cm of DBH), hotspots and coldspots of error accounted for the highest rate, with 86.46% and 77.33%, respectively. It demonstrates the concentration of error because the boundary of tree crowns in the satellite images is not divided; there is information about the texture of trees, but not about height. Also, it could be the reason that the tree was too small to be reflected from stand-level forests in the two-dimensional satellite imageries.

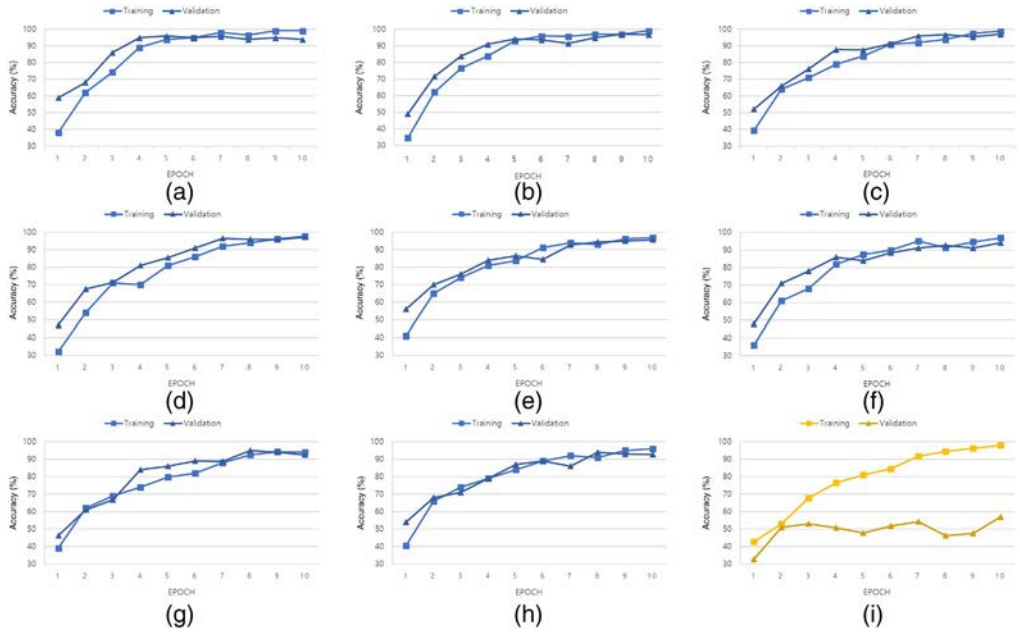

Fig. 6 Comparison of accuracy results according to training, validation and test data set ratios I: (a) 90% training, 10% validation and test, (b) 80% training, 20% validation and test, (c) 70% training, 30% validation and test, (d) 60% training, 40% validation and test, (e) 50% training, 50% validation and test, (f) 40% training, 60% validation and test, (g) 30% training, 70% validation and test, (h) 20% training, 80% validation and test, and (i) 10% training, 90% validation and test.

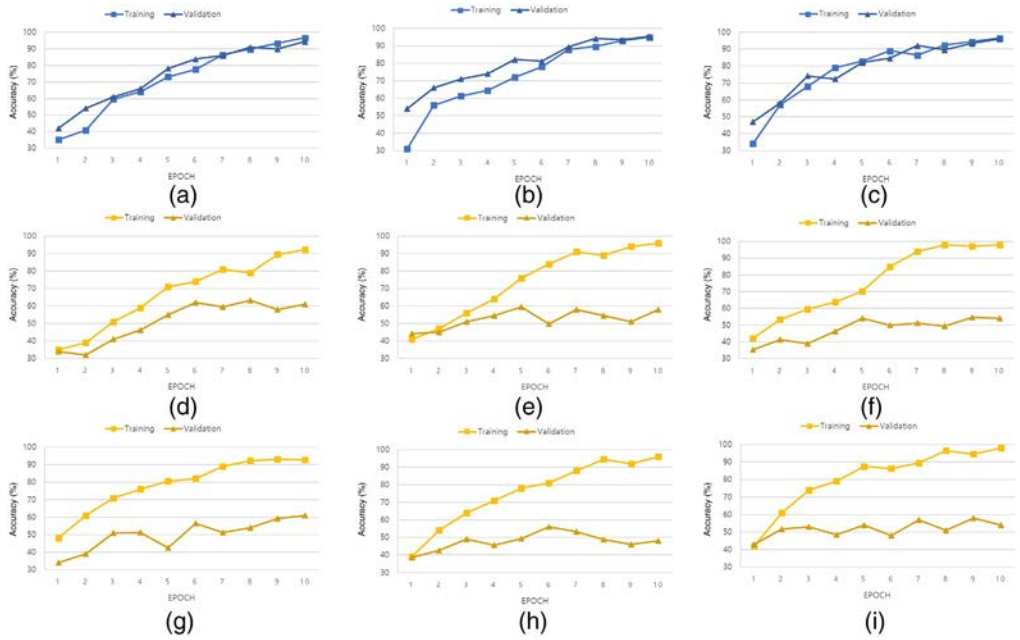

Fig. 7 Comparison of accuracy results according to training, validation and test data set ratios II: (a) 19% training, 81% validation and test, (b) 18% training, 82% validation and test, (c) 17% training, 83% validation and test, (d) 16% training, 84% validation and test, (e) 15% training, 85% validation and test, (f) 14% training, 86% validation and test, (g) 13% training, 87% validation and test, (h) 12% training, 88% validation and test, and (i) 11% training, 89% validation and test.

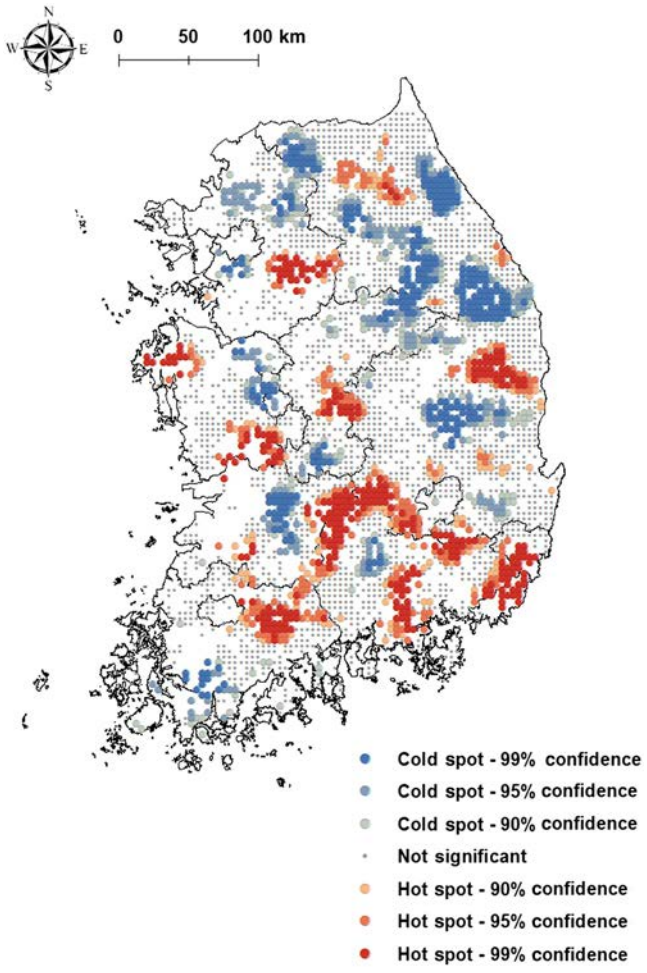

Fig. 8 Hotspot of stand volume estimation errors, from 17% training and 83% estimation.

Table 2 Distribution of hotspots and coldspots by DBH class.

Class	Range	The number of underestimated values (number of error hotspots/ total number of error hotspots)	Rate of hotspot distribution (%)	The number of overestimated values (number of error coldspots/ total number of error coldspots)	Rate of coldspot distribution (%)
DBH (cm)	0 to 16	249/288	86.46	249/322	77.33
	16 to 30	38/288	13.19	70/322	21.74
	~30	1/288	0.35	3/322	0.93

4 Discussion

The CNNs model, which was applied to estimate stand volume based on NFI and other satellite data, needs to be validated through the previous literature. Because the overall spatial characteristics were analyzed through the clustering, the value of stand volume also should be the range of other stand volume estimations. Therefore, the other estimated value of stand volume from other estimations using satellite imagery and other spatio-temporal modeling were compared. Some study sites had many field studies as well as modeling results of stand volume, so we could compare the results with them directly. Even though the satellite imageries or geospatial information used in each research may be different, the accuracy of stand volume estimation can be directly compared by methodologies. Therefore, the R^2 values were adopted to understand our modeling results. When we compared our results with the satellite-based previous literature, R^2 for stand volume estimates were calculated from 0.53 to 0.81, depending on the learning rate of CNNs (Table 3). Furthermore, when using 17% NFI data for training, the total stand volume of South Korea was distributed as 709.04 Mm^3 (R^2 ¼ 0.96).

Table 3 Comparing CNNs model and previous literature.

Category	Model	Value	Sources	Locations
Estimated R^2	CNNs	0.93 to 0.96	This study	South Korea
	Direct linear regression	0.53	Ref. 30	Hunan, China
	Logarithmic regression	0.60		
	Quadratic regression	0.60		
	Exponential regression	0.58		
	Water-cloud analysis regression	0.61		
	Multivariable regression	0.67		
	CNNs, Nonlinear mixed effects regression	0.81	Ref. 31	Daxing'anling, China
Stand volume ($m3\ ha^{-1}$)	CNNs	124.62 to 127.85	This study	South Korea
	CBM-CFS3	125.6	Ref. 32	
	Forest growth	126.73	Ref. 33	

Reference 30 estimates stand volume using the synthetic approach radar images. Direct linear, logarithmic quadratic exponential, water-cloud analysis, multivariate regression models were used as methodologies with R^2 results of 0.53 to 0.67.

Reference 31 used CNNs to estimate stand volume after performing species classification, with R^2 derived up to 0.81. Besides, using the nonlinear mixed-effects model, to solve the interface of the mixed forest and the interspecies effect on the stand volume estimation.

Stand volume derived from this study was found to be in a fairly similar range, 126.73 and 125.6 $m^3\ ha^{-1}$, respectively, in the study using the forest growth model and the CBM-CFS3 model [32,33].

This study is meaningful in that it can be estimated stand volume using deep learning for forests in South Korea. We have identified the minimum portion of the forest field survey area required to estimate the entire stand volume. Some studies in Table 3, the accuracy of the model (R^2) and the amount of estimated stand volume were improved by using

LiDAR and RADAR; however, in this study, it is meaningful in that the accuracy of the model was improved only with optical images and geospatial information. Also, it was estimated to be similar to the model performance of the other studies. If additional information, such as satellite images with a hyper-spectral sensor and height information, are used in the CNNs model, the estimated accuracy for stand volume will increase. However, it is difficult to estimate the underground biomass by using only remotely sensed data. Thus, to estimate the total biomass for the entire forest, more spatial information in terms of underground forests should be further considered.

Forest stand volume is increased from 20.57 to 239.85 Tg C in the past five decades in South Korea [34]. In South Korea, forest statistics at the county level have been estimated based on the NFI field data. Because the NFI data were designed for the national-level inventory, only generalized or limited forest statistics are available for the small areas based on the NFI field data. CNNs can support more specific information at the local scale, it is common to conduct an additional field survey or use a complicated data analysis procedure [35]. Small-area estimation forest inventory is a statistical approach for the estimation of characteristics without additional field surveys for a small subpopulation that was not specifically targeted in the sampling design [36]. For small-area estimation, calibration techniques use samples surveyed outside an area of interest to produce estimates for the area of interest.

This result proves the CNNs algorithm for stand volume map based on 17% training with 83% validation has relatively high accuracy. This method indicates the higher the training sample increases the quality of the map and as well as the high accuracy of forest stand volume estimation of large-scale Forest inventories. The estimates of the present study indicate considering a large training sample enhances the accuracy as it is based on a function of stand volume density for the entire forest of South Korea. Therefore, CNNs may also be able to address the issue of forest inventories, especially for individual tree segmentation. CNNs have been enormously effective at segmenting objects from photographic and video imagery. Most CNN-based segmentation algorithms work by identifying potential bounding boxes of objects and then analyzing the interior of those bounding boxes to assess their validity. We believe that a similar algorithm could be adapted to identify the 3D bounding boxes of individual trees. Another CNN-based segmentation method known as semantic segmentation seeks to isolate individual pixels that represent the desired object [37].

5 Conclusions

We found that using CNNs model based on satellite imageries and geospatial information is considered to be suitable for estimating the national level of stand volume. Compared with previous studies, our estimate provides another means of assessing forest stand volume by using a deep learning algorithm in South Korean forests. Although there are uncertainties in the estimates, these are expected to decrease as more accurate field survey data become available and remote sensing technologies are developed. Besides, further research is needed to understand the weight of input data to minimize the cost of collecting uninfluential data. This study is meaningful in that we (1) estimated the stand volume with a deep learning algorithm, (2) identified the minimum training rate of the CNNs model to estimate the stand volume of the entire South Korean forest, and (3) identified the effect of diameter class on error hotspots in stand volume estimates through clustering analysis.

6 Appendix A

6.1 *Scenarios Considering the Percentage of Training, Validation, and Test Data Set for CNNs Model*

Training, validation, and test rate used in the CNNs model for each scenario was presented in Table 4.

Table 4 Detailed percentage of the CNNs model's training, validation, and test data set.

Scenario	Training rate (%)	Validation rate (%)	Test rate (%)
1	90	5	5
2	80	10	10
3	70	15	15
4	60	20	20
5	50	25	25
6	40	30	30
7	30	35	35
8	20	40	40
8-1	19	40.5	40.5
8-2	18	41	41
8-3	17	41.5	41.5
8-4	16	42	42
8-5	15	42.5	42.5
8-6	14	43	43
8-7	13	43.5	43.5
8-8	12	44	44
8-9	11	44.5	44.5
9	10	45	45

6.2 *Statistics of Forest Stand Volume in South Korea*

Table 5 shows average, maximum, minimum, total stand volume, and standard deviation of the results for CNNs model based on training rate.

Table 5 Detailed CNNs model statistics by training rate.

Training rate (%)	Average stand volume ($m^3 ha^{-1}$)	Maximum stand volume ($m^3 ha^{-1}$)	Minimum stand volume ($m^3 ha^{-1}$)	Standard ($m^3 ha^{-1}$)	Total stand volume (Mm^3)
100	127.85	275.71	21.47	35.16	727.42
90	127.07	279.99	22.10	34.58	722.98
80	127.25	274.76	21.81	33.85	724.01
70	127.92	278.58	19.46	33.44	728.10
60	128.56	276.91	22.03	32.78	731.46
50	128.03	274.28	15.41	33.06	728.44
40	126.58	277.69	22.34	31.53	720.19
30	125.36	278.23	21.62	34.87	713.25
20	125.93	280.18	13.24	37.98	716.50
19	125.84	269.01	25.49	34.00	715.98
18	124.57	274.69	26.55	30.76	708.75
17	124.62	275.43	26.42	30.77	709.04
16	115.32	257.03	20.88	31.01	656.13
15	110.07	252.27	14.90	32.14	626.26
14	108.93	251.97	11.63	33.13	619.77
13	109.01	252.63	10.36	32.59	620.23
12	107.16	256.72	14.78	34.32	609.70
11	105.71	247.92	8.97	32.40	601.45
10	103.26	247.74	12.75	33.40	587.51

Acknowledgments

The authors would like to thank the anonymous reviewers and editorial staff for their comments, which greatly improved this manuscript. This study was developed in the Young Scientists Summer Program (YSSP) at the International Institute for Systems Analysis (IIASA), Laxenburg (Austria), supported by the Korea Agency for Infrastructure Technology Advancement (KAIA) grant funded by the Ministry of Land, Infrastructure, and Transport (22UMRG-C158200-03). The authors declare no conflicts of interest.

Code, Data, and Materials Availability

Cha, Sungeun (2022), Datasets for running Convolutional Neural Networks (CNNs), Dryad, Dataset, The online version contains supplementary material at https://doi.org/10.5061/dryad.jdfn2z3b5.

References

1. R. T. Watson et al., *Land Use, Land-Use Change and Forestry: A Special Report of the Intergovernmental Panel on Climate Change*, Cambridge University Press, Cambridge, England (2000).
2. Korea Forest Service (KFS), *Statistical Yearbook of Forestry*, Republic of Korea (2017).
3. T. G. Cole and J. J. Ewel, "Allometric equations for four valuable tropical tree species," *For. Ecol. Manage.* 229(1–3), 351–360 (2006).
4. J. Perman, "Good practice guideline for land use, land-use change and forestry," Intergovernmental Panel on Climate Change (IPCC) (2003).
5. Korea Forest Research Institute (KFRI), "The 5th National Forest Inventory report," Republic of Korea (2011).
6. B. S. Kim, "The final report for statistics quality management of national forest inventory in 2008," Korea National Statistical Office (KOSTAT), Republic of Korea (2008).
7. M. Katila and E. Tomppo, "Stratification by ancillary data in multisource forest inventories employing k-nearest-neighbour estimation," *Can. J. For. Res.* 32(9), 1548–1561 (2002).
8. H. J. Lee et al., "Analysis of satellite images to estimate forest biomass," *J. Korean Soc. Geospat. Inf. Syst.* 21(3), 63–71 (2013).
9. H. J. Lee and J. H. Ru, "Application of LiDAR data & high-resolution satellite image for calculate forest biomass," *J. Korean Soc. Geospat. Inf. Sci.* 20(1), 53–63 (2012).
10. D. Haboudane et al., "Integrated narrow-band vegetation indices for prediction of crop chlorophyll content for application to precision agriculture," *Remote Sens. Environ.* 81(2–3), 416–426 (2002).
11. K. Tan et al., "Satellite-based estimation of biomass carbon stocks for northeast China's forests between 1982 and 1999," *For. Ecol. Manage.* 240(1-3), 114–121 (2007).
12. Korea Forest Service (KFS), "6th basic forest plan," Republic of Korea (2018). 13. Y.

LeCun et al., "Deep learning," *Nature* 521(7553), 436–444 (2015).

14. E. Ayrey and D. J. Hayes, "The use of three-dimensional convolutional neural networks to interpret LiDAR for forest inventory," *Remote Sens.* 10(4), 649 (2018).
15. H. Noh et al., "Learning deconvolution network for semantic segmentation," in *Proc. IEEE Int. Conf. Comput. Vision*, pp. 1520–1528 (2015).
16. H. Guan et al., "Deep learning-based tree classification using mobile LiDAR data," *Remote Sens. Lett.* 6(11), 864–873 (2015).
17. B. N. Narayanan et al., "Support vector machine and convolutional neural network based approaches for defect detection in fused filament fabrication," *Proc. SPIE* 11139, 1113913 (2019).
18. Korea Forest Service (KFS), *Statistical Yearbook of Forestry*, Republic of Korea (2017).
19. S. R. Kim et al., "Forest cover classification by optimal segmentation of high resolution satellite imagery," *Sensors* 11(2), 1943–1958 (2011).
20. J. Penman et al., "Good practice guidance for land use, land-use change and forestry" (2003).
21. J. Jung et al., "Estimation of aboveground forest biomass carbon stock by satellite remote sensing—a comparison between k-nearest neighbor and regression tree analysis," *Korean J. Remote Sens.* 30(5), 651–664 (2014).
22. Y. LeCun et al., "Gradient-based learning applied to document recognition," *Proc. IEEE* 86(11), 2278–2324 (1998).

23. P. Savarese and M. Maire, "Learning implicitly recurrent CNNs through parameter sharing," arXiv:1902.09701 (2019).
24. A. Getis, "Spatial autocorrelation," *Handbook of Applied Spatial Analysis*, pp. 255–278, Springer, Berlin, Heidelberg (2010).
25. L. Anselin and S. J. Rey, "Perspectives on spatial data analysis," *Advances in Spatial Science*, pp. 1–20, Springer, Berlin, Heidelberg (2010).
26. K. A. Brown et al., "Predicting plant diversity patterns in Madagascar: understanding the effects of climate and land cover change in a biodiversity hotspot," *PLoS One* 10(4), e0122721 (2015).
27. C. F. Cáceres, "Using GIS in hotspots analysis and for forest fire risk zones mapping in the Yeguare region, southeastern Honduras," Papers in Resource Analysis, Vol. 13, pp. 1–14 (2011).
28. Korea Forest Service (KFS), "Forest resource business plan for 2018," Republic of Korea (2018).
29. M. C. de Castro and B. H. Singer, "Controlling the false discovery rate: a new application to account for multiple and dependent tests in local statistics of spatial association," *Geog. Anal.* 38(2), 180–208 (2006).
30. H. Zhang et al., "Forest growing stock volume estimation in subtropical mountain areas using PALSAR-2 L-band PolSAR data," *Forests* 10, 276 (2019).
31. J. Liu et al., "Classification of tree species and stock volume estimation in ground forest images using deep learning," *Comput. Electron. Agric.* 166, 105012 (2019).
32. M. Kim et al., "Estimating carbon dynamics in forest carbon pools under IPCC standards in South Korea using CBM-CFS3," *iForest-Biogeosci. For.* 10, 83–92 (2017).
33. K. Nam et al., "Spatio-temporal change in forest cover and carbon storage considering actual and potential forest cover in South Korea," *Sci. China Life Sci.* 58(7), 713–723 (2015).
34. X. Li et al., "Forest biomass carbon accumulation in Korea from 1954 to 2007," *Scand. J. For. Res.* 25(6), 554–563 (2010).
35. J. S. Yim et al., "Comparison of the k-nearest neighbor technique with geographical calibration for estimating forest growing stock volume," *Can. J. For. Res.* 41(1), 73–82 (2011).
36. J. N. Rao, "Small-area estimation," in *Wiley StatsRef: Statistics Reference Online*, pp. 1–8, John Wiley & Sons, In., New Jersey (2015).
37. N. Karianakis et al., "Boosting convolutional features for robust object proposals," arXiv: 1503.06350 (2015).